

# Polymer-Encapsulated Carbon Nanotubes Prepared through Ultrasonically Initiated In Situ Emulsion Polymerization

Hesheng Xia, Qi Wang,\* and Guihua Qiu

State Key Laboratory of Polymer Materials Engineering, Polymer Research Institute, Sichuan University, Chengdu 610065 China

Received March 22, 2003. Revised Manuscript Received July 25, 2003

In this study, a novel ultrasonically initiated in situ emulsion polymerization approach was used to modify multi-walled carbon nanotubes (MWCNTs). The dispersion behavior of MWCNTs in aqueous solution under ultrasonic irradiation was investigated by spectrophotometry. Ultrasonically initiated emulsion polymerization of monomer *n*-butyl acrylate (BA) and methyl methacrylate (MMA) are reported. By employing the multiple effects of ultrasound, i.e., dispersion, pulverizing, activation, and initiation, the aggregation and entanglement of carbon nanotubes in aqueous solution can be broken down, while in situ polymerization of monomer BA or MMA on the surface of MWCNTs proceeds without any added chemical initiator; consequently, the MWCNTs are coated by the formed polymer. Transmission electron microscopy confirms that after surface modification through ultrasonically initiated in-situ polymerization, the size of MWCNTs increased; even after 72 h of Soxhlet extraction with boiling acetone there are still unextracted polymers in the modified MWCNTs, indicating strong interaction between the polymer and carbon nanotubes. The results of thermogravimetric analysis show that there are high encapsulation rates for PBA. The characteristic peak of C=O in carbonyl groups at  $\sim 1733\text{ cm}^{-1}$  still appears in the Fourier transform infrared spectrum of the extracted polymer-encapsulated MWCNTs. X-ray photoelectron spectroscopy further confirms the presence of polymer-encapsulated MWCNTs and strong interaction between polymer and MWCNTs. Therefore, ultrasonically initiated in situ emulsion polymerization provides a novel surface modification method for carbon nanotubes. The polymer-encapsulated carbon nanotubes can be well dispersed in Nylon 6 matrix. The interface adhesion between polymer-encapsulated carbon nanotubes and Nylon 6 is improved. The yield strength is improved  $\sim 30\%$  and the Young's modulus is improved  $\sim 35\%$  at only 1 wt % content of polymer-encapsulated carbon nanotubes.

## Introduction

Carbon nanotubes (CNTs)/polymer composites have attracted much attention recently.<sup>1–5</sup> Carbon nanotubes are ideal reinforcing fibers for composites because they have high aspect ratio, high mechanical strength, and high electrical and thermal conductivity. Also, compared to the conventional carbon fiber or glass fiber with a large size, carbon nanotubes/polymer composite are easily molded, and the shaped plastic articles have perfect surface appearance. However, the big challenges encountered in making such a composite are (i) uniform dispersion of CNTs in polymer matrix without aggregation and entanglement, and (ii) improved nanotubes/resin interface adhesion. One way to solve these problems is to modify the surface properties by introducing

some functional groups such as  $-\text{OH}$ ,  $-\text{COOH}$ ,  $-\text{C}=\text{O}$ , etc. Because carbon nanotubes cannot be melted and are difficult to dissolve in common solvents, it is difficult to attain chemical modification and functionalization of carbon nanotubes. Several studies on chemical modification of CNTs have been reported. Chen reported an approach to the dissolution of shortened single-walled carbon nanotubes (SWNTs) in common organic solvents by derivation of SWNTs with thionyl chloride and octadecylamine, and further explored the functionalization of soluble SWNTs by reacting the soluble SWCNTs with dichlorocarbene.<sup>6</sup> Wong reported modification of multiwall carbon nanotubes via amide bond formation between carboxyl functional groups bonded to the open ends of MWCNTs and amine.<sup>7</sup> Mickelson reported the chemical modification of SWCNTs side-walls by fluorination, which was performed by heating purified SWCNTs in fluorine.<sup>8</sup> Generally, the chemical modifications of carbon nanotubes mentioned above

\* To whom correspondence should be addressed. E-mail: qiwang@scu.edu.cn. Fax: +86-28-85402465. Tel: +86-28-85405133.

(1) Ajayan, P. M.; Stephan, O.; Colliex, C.; Tranth, D. *Science* **1994**, *265*, 1212.

(2) Calvert, P. *Nature* **1999**, *399*, 210.

(3) Gong, X.; Liu, J.; Baskran, S.; Voise, R. D.; Young, J. S. *Chem. Mater.* **2000**, *12*, 1049.

(4) Thostenson, E. T.; Ren, Z. F.; Chou, T.W. *Composite Sci. Technol.* **2001**, *61*, 1899.

(5) Shaffer, M. S. P.; Windle, A. H. *Adv. Mater.* **1999**, *11*, 937.

(6) Chen, J.; Hamon, M. A.; Hu, H.; et al. *Science* **1998**, *282*, 95.  
(7) Wong, S. S.; Joselevich, E.; Woolley, A. T.; Cheung, C. L.; Lieber, C. M. *Nature* **1998**, *394*, 52.  
(8) Mickelson, E. T.; Huffman, C. B.; Rinzler, A. G.; Smalley, R. E.; Hauge, R. H.; Margrave, J. L. *Chem. Phys. Lett.* **1998**, *296*, 188.

were attained through the oxidation of carbon nanotubes in concentrated  $\text{H}_2\text{SO}_4$  and  $\text{HNO}_3$  solution, but under such harsh acidic media the walls of carbon nanotubes can be broken. And these approaches require a series of complicated chemical reactions on the surface of the carbon nanotubes. Also, the introduction of the functional groups is not enough to separate and stabilize the carbon nanotubes.

Encapsulating carbon nanotubes with polymer as an alternative approach can be used to realize the surface modification. Koshio attained the chemical modification of SWCNTs by ultrasonically treating them in a monochlorobenzene (MCB) solution of poly(methyl methacrylate) PMMA.<sup>9</sup> O'Connell prepared poly(vinylpyrrolidone) (PVP) wrapped SWCNTs by treating the SWCNTs and a PVP aqueous dispersion with high-shear mixing and sufficient ultrasonication.<sup>10</sup> Tang employed in situ catalyzed polymerization to prepare poly(phenylacetylenes) wrapped MWCNTs. Shearing of poly(phenylacetylenes) wrapped MWCNTs solutions readily aligns the nanotubes along the direction of the applied mechanical force.<sup>11</sup> Blau prepared poly(*m*-phenylenevinylene-*co*-2,5-dioctyloxy-*p*-phenylenevinylene) (PmPV) wrapped carbon nanotubes by simple mixing in a solution of PmPV in toluene and characterized the interaction between conjugated polymer and carbon nanotubes by TEM and spectroscopic measurement.<sup>12</sup> To our knowledge, few reports involve in the emulsion polymerization method to modify the carbon nanotubes. In this study we propose an ultrasonically initiated in situ emulsion polymerization method to prepare polymer-encapsulated carbon nanotubes.

Ultrasonic irradiation, as a new technology, has been widely used in chemical synthesis.<sup>13</sup> When an ultrasonic wave passes through a liquid medium, a large number of microbubbles form, grow, and collapse in very short time of about a few microseconds, an effect which is called ultrasonic cavitation. Sonochemical theory calculations and the corresponding experiments suggested that ultrasonic cavitation can generate local temperature as high as 5000 K and local pressure as high as 500 atm, with a heating and cooling rate greater than  $10^9$  K/s, a very rigorous environment.<sup>14</sup> Therefore, ultrasound has been extensively applied in dispersion, emulsifying, crushing, and activation of particles. Previously we prepared polymer-encapsulated spherical inorganic nanoparticles through ultrasonic irradiation.<sup>15-17</sup> In the present study, by taking advantage of the multi-effect of ultrasound, the aggregates and entanglement of carbon nanotubes can be broken down. The in-situ

polymerization of monomer BA or MMA proceeds while carbon nanotubes are redispersed by ultrasound. This method has the following advantages: (i) use of aqueous media, (ii) ease of operation, and (iii) ability to design the encapsulated polymer layer to meet different requirements. In addition, we employed the polymer encapsulated carbon nanotubes to prepare Nylon 6/carbon nanotubes composites. The dispersion of carbon nanotubes in Nylon 6 matrix and the mechanical properties of the composites were studied.

## Experimental Methods

**Materials.** MWCNTs were provided by Chengdu Institute of Organic Chemistry, Chinese Academy of Sciences. MWCNTs were synthesized by dissociation of methane at high temperature with a  $\text{NiO/La}_2\text{O}_3$  catalyst. The outer diameter of MWCNTs was  $\sim 20$  nm, and the inner diameter was 5–10 nm. The products were washed with concentrated hydrochloric acid to remove the catalyst and the carrier of catalyst, and then were purified with concentrated  $\text{HNO}_3$  to remove the amorphous carbon particles. Nylon 6 (PA 6) in pellet form (relative viscosity  $\sim 3.2$  in 98%  $\text{H}_2\text{SO}_4$  solvent, and diameter 2–3 mm) was supplied by Yueyang Petro-Chemical Engineering Factory. *n*-Butyl acrylate (BA) and methyl methacrylate (MMA) were from Tianjin Chemical Reagent Factory. BA and MMA were washed 3  $\times$  with a 10% aqueous solution of sodium hydroxide and distilled water to remove the inhibitor hydroquinone, dried with anhydrous sodium sulfate, then vacuum distilled. Sodium lauryl sulfonate (SLS) was obtained from the Shanghai Xiangde Chemical Factory, China.

**Apparatus.** The reaction apparatus was described in a previous paper.<sup>15</sup> The ultrasonic irradiation instrument was a VC-1500 (Sonic & Material Co.) equipped with the following: standard titanium horn with a diameter of 22 mm, adjustable power output, replaceable flat stainless steel tip, digital thermometer to determine temperature, and gas flow meter to measure gas flow rate. The glass reactor was self-designed and made in house.

**Ultrasonically Initiated In Situ Emulsion Polymerization in the Presence of Carbon Nanotubes.** The polymerizations were conducted according to the following procedures. First, 1.0 g of MWCNTs, 0.4 mL of BA or MMA, and 100 mL of 0.5% SLS aqueous solution were introduced into the reaction vessel. Second, the mixture was deoxygenated by bubbling it with oxygen-free nitrogen for 2 min in the reaction vessel, and water was circulated to maintain a temperature of 30 °C. Ultrasonic irradiation was then carried out with the probe of the ultrasonic horn immersed directly into the mixture emulsion system. The power output was set at 600 W and the  $\text{N}_2$  flow rate was 12 mL/min. A thermistor probe was immersed into the solution to measure the temperature variation during polymerization. After 30 min of irradiation the reaction was stopped. Finally, the prepared emulsions were de-emulsified with ice-cold methanol, then the precipitated mixtures were filtered, washed, vacuum-dried at 70 °C, and weighed to ascertain the conversion gravimetrically in the usually way. Also, ultrasonically initiated emulsion polymerization in the absence of carbon nanotubes was conducted. The experimental procedures were the same.

**Preparation of PA6/Carbon Nanotubes Composites.** First, 200 g of PA6 was dried at 100 °C for 48 h in a vacuum prior to blending. Dried PA6 (200 g) and 2 g of polymer-encapsulated MWCNTs or raw MWCNTs were melt-blended by using a Haake Screw Twin Extruder (Haake Co., Germany) at process zone temperature between 235 and 250 °C. The rotating speed of the screws was kept at 30 rpm. The extruded blends were stranded, cooled, and pelletized. Blend pellets were dried at 100 °C for 48 h in a vacuum, and then injection molded into standard tensile and impact specimens at process zone temperature between 220 and 250 °C with a K-TEC 40 model injection molding machine (Terromatic, Milacron Co., Cincinnati, OH).

(9) Koshio, A.; Yudasaka, M.; Zhang, M.; Iijima S. *Nano Lett.* **2001**, *1*, 361.

(10) O'Connell, M. J.; Boul, P.; Ericson, L. M.; Huffman, C.; Wang, Y.; et al. *Chem. Phys. Lett.* **2001**, *342*, 265.

(11) Tang, B. Z.; Xu, X. *Macromolecules* **1999**, *32*, 2569.

(12) McCarthy, B.; Coleman J. N.; Czerw, R.; Dalton, A. B.; in het Panhuis, M.; Maiti, A.; Drury, A.; Bernier, P.; Nagy, J. B.; Lahr, B.; Byrne, H. J.; Carroll, D. L.; Blau, W. J. *J. Phys. Chem. B* **2002**, *106*, 2210.

(13) Mason, T. J.; Lorimer, J. P. *Sonochemistry: Theory, Applications and Uses of Ultrasound in Chemistry*; Ellis Horwood: Chichester, UK, 1988.

(14) Suslick, K. S. *Science* **1990**, *3*, 1439.

(15) Wang, Q.; Xia, H. S.; Zhang, C. H. *J. Appl. Polym. Sci.* **2001**, *80*, 1478.

(16) Xia, H. S.; Zhang, C. H.; Wang, Q. *J. Appl. Polym. Sci.* **2001**, *80*, 1130.

(17) Xia, H. S.; Wang, Q. *Chem. Mater.* **2002**, *14*, 2158.

**Characterization.** The dispersion of carbon nanotubes in aqueous solution was evaluated by the determination of absorption at 500 nm. The sample was prepared as follows. A 0.1-g portion of carbon nanotubes was added to 80 mL of surfactant aqueous solution, then the suspension was subjected to ultrasonic irradiation at power output of 600 w for 5 min. Then the 15-mL dispersion was centrifuged for 20 min at 4000 rpm. The 0.5-mL upper dispersion was withdrawn and diluted to 25 mL; the absorption of the diluted suspension at 500 nm was determined by spectrophotometry with a 721 model spectrophotometer. The higher the absorption is, the better the dispersion of carbon nanotubes is.

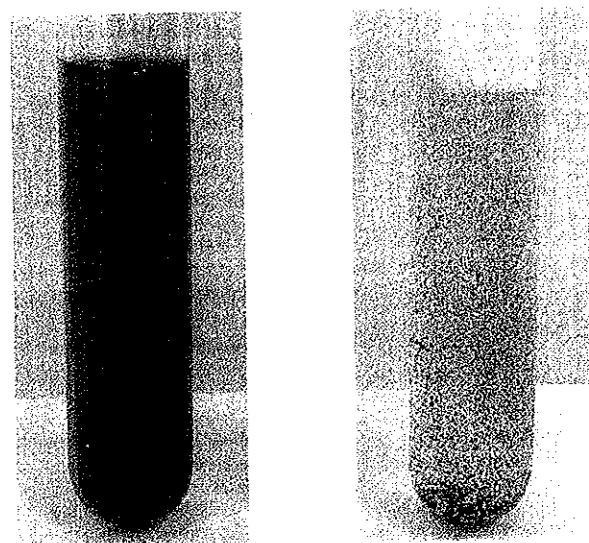
To characterize the strength of the interaction between polymer and MWCNTs, the synthesized polymer/MWCNTs composites were wrapped with filter paper with a pore diameter of  $\sim 100$  nm, then extracted 72 h with a Soxhlet extractor with boiling acetone (the homopolymer is thought to be completely removed by this way). Fourier transform infrared (FTIR) spectra of the composites in KBr pellets were recorded on a Nicolet 560 FTIR spectrometer. The spectra were collected from 4000 to 400  $\text{cm}^{-1}$ , with a 4  $\text{cm}^{-1}$  resolution over 20 scans. Thermogravimetric analysis (TGA) of the polymer was carried out on a General V 4.1c Dupont TA2100 instrument thermal analyzer with a heating rate of 10  $^{\circ}\text{C}/\text{min}$  from room temperature to 750  $^{\circ}\text{C}$  and a dynamic nitrogen flow of 50  $\text{cm}^3\cdot\text{min}^{-1}$ . The particle morphology of all the samples was observed by TEM on a JEM 100-CX instrument with an accelerating voltage of 20 kV. The average diameters of nanotubes were estimated by counting at least 20 tubes in the TEM photos. The raw MWCNTs and the extracted polymer-encapsulated MWCNTs were redispersed respectively in acetone with ultrasonic bath and then the dispersion was dropped on a copper grid to observe the morphology of MWCNTs. X-ray photoelectron spectroscopy (XPS) was performed on an XSAM 800 X-ray photoelectron spectrometer with a Mg K $\alpha$  X-ray source (1253.6 eV). The X-ray source was run at a reduced power of 120 w (12 kV and 10 mA). The polymer-encapsulated MWCNTs or raw MWCNTs were pressed at 600 atm into a pellet for testing. The pressure in the analysis chamber was maintained at  $10^{-8}$  mbar during the measurements. In the data analysis, to compensate for surface-charging effects, all binding energies (BE) were referred to the core level C $_{1s}$  of raw MWCNTs at 284.3 eV. The surface elemental stoichiometries were determined from the ratios of peak areas corrected with the empirical sensitivity factors, and is liable to  $\pm 5\%$  error.

Tensile properties were tested, following ASTM D-638, by using a material tester (Instron 4302, UK) at a crosshead speed of 100 mm/min. Izod notched impact strength was tested according to ASTM D-256 by using an impact strength tester (XJ-40A, China). The phase morphology was characterized with a scanning electromicroscope (SEM) (Hitachi X-650, Japan). Standard specimens were cryogenically fractured in liquid nitrogen. The fractured surface was sputter-coated with gold before observation.

## Results and Discussion

### Ultrasonic Dispersion of Carbon Nanotubes.

From Figure 1, it can be seen that high-intensity ultrasound has an excellent dispersion effect for carbon nanotubes in aqueous solution. The 0.1 wt % carbon nanotubes and 0.1 wt % surfactant aqueous suspensions become homogeneous dispersions after 2 min of ultrasonic irradiation (Figure 1 a). As a contrast, the 0.1 wt % carbon nanotubes and 0.1 wt % surfactant SLS aqueous suspensions remain undispersed even after 1 h of conventional stirring at a rate of 400 rpm, and the suspended coagulates of carbon nanotubes can be clearly seen without magnification (Figure 1 b). Also, we examined the effect of surfactant on the dispersion of carbon nanotubes in aqueous dispersion.



Ultrasonic irradiation  
Time: 2 min  
Power: 600 W

Conventional stirring  
Time: 1 hr  
Stirring rate: 400 rpm

Figure 1. Dispersion of 0.1 wt % MWCNTs in 0.1 wt % SLS aqueous suspension.

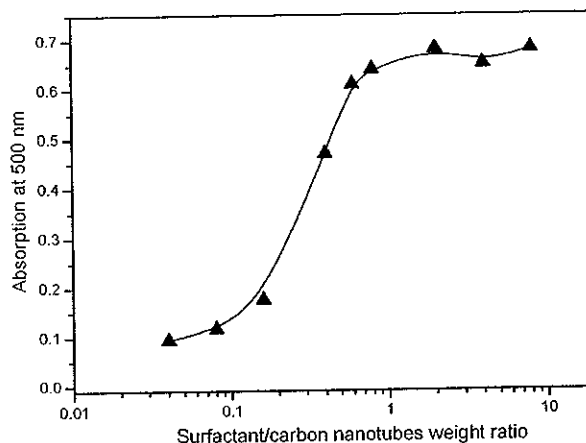
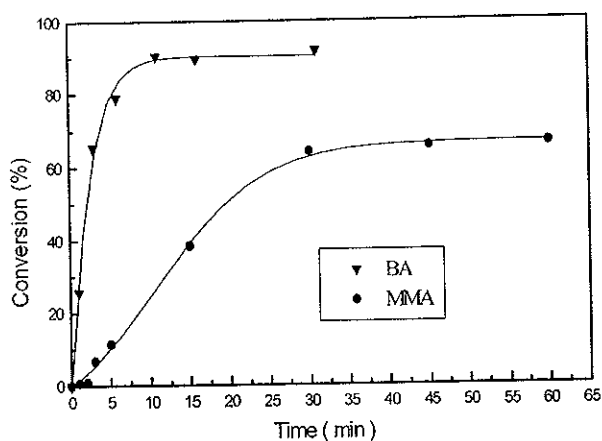


Figure 2. Effect of surfactant/MWCNTs weight ratio on the dispersion of MWCNTs in the diluted aqueous dispersions.

Figure 2 shows the effect of surfactant SLS/carbon nanotubes weight ratio on the dispersion of carbon nanotubes in the diluted aqueous dispersions. From Figure 2, it can be seen that with the increase of surfactant concentration, the absorption at 500 nm increases; when surfactant/carbon nanotubes weight ratio ( $S/C$ ) increases to a value, the absorption at 500 nm remains nearly unchanged, suggesting that the good dispersion is attained. The minimum  $S/C$  value for the good dispersion is 0.8 for SLS.

**Ultrasonically Initiated Emulsion Polymerization.** The premise of ultrasonically initiated encapsulating emulsion polymerization of monomer is that ultrasound can initiate polymerization of monomers without any chemical initiator. As shown in Figure 3, the conversion of monomer BA amounts to 91% in 11 min, and the conversion of monomer MMA amounts to 65% in 30 min. As mentioned above, ultrasonic cavitation can generate local high temperature and pressure, a



**Figure 3.** Time-conversion curves of ultrasonically initiated emulsion polymerization of monomer MMA and BA. (BA concentration 10% (v/v), SLS concentration 1 wt %, bath temperature 45 °C, N<sub>2</sub> flow rate 12 mL/min, power output 110 W).

very rigorous environment for chemical reaction. Under these rigorous conditions radicals can be generated due to decomposition of water, monomer, or surfactant, or rupture of polymer chains to initiate the polymerization of monomer.<sup>18,19</sup>

**Polymer-Encapsulated Carbon Nanotubes Prepared through Ultrasonically Initiated In Situ Emulsion Polymerization.** Polymer-encapsulated carbon nanotubes were prepared through ultrasonically initiated in-situ emulsion polymerization in the presence of carbon nanotubes. The polymerization of monomer was initiated by ultrasonic cavitation, and the in situ emulsion polymerization proceeded during ultrasonic dispersion. The prepared polymer-encapsulated carbon nanotubes were characterized by TEM, TGA, FTIR, and XPS. In this case, the surfactant SLS was chosen because it not only has a good dispersion effect for carbon nanotubes, but also favors ultrasonic initiation compared with other surfactants such as poly(ethylene glycol) mono-4-octylphenyl ether (OP).

TEM photographs of raw MWCNTs and PBA-encapsulated MWCNTs after Soxhlet extraction are shown in Figure 4. The average diameter of the raw MWCNTs (Figure 4 a) is ~20 nm. Figure 4 b shows that after 72 h of Soxhlet extraction with boiling acetone, the average diameter of the encapsulated MWCNTs increased to ~30 nm. The results suggest that after ultrasonically initiated in situ polymerization in the presence of carbon nanotubes, PBA is closely coated on the sidewall of MWCNTs.

The TGA curves of raw MWCNTs, PBA, or PMMA-encapsulated MWCNTs before and after 72 h of Soxhlet extraction with acetone are shown in Figure 5. The raw carbon nanotubes do not decompose before 600 °C as shown in curve a of Figure 5. For the polymer-encapsulated MWCNTs, the polymer part will completely decompose before 500 °C. The polymer content in polymer-encapsulated MWCNTs can be calculated through the TGA method. As shown in Table 1, it is

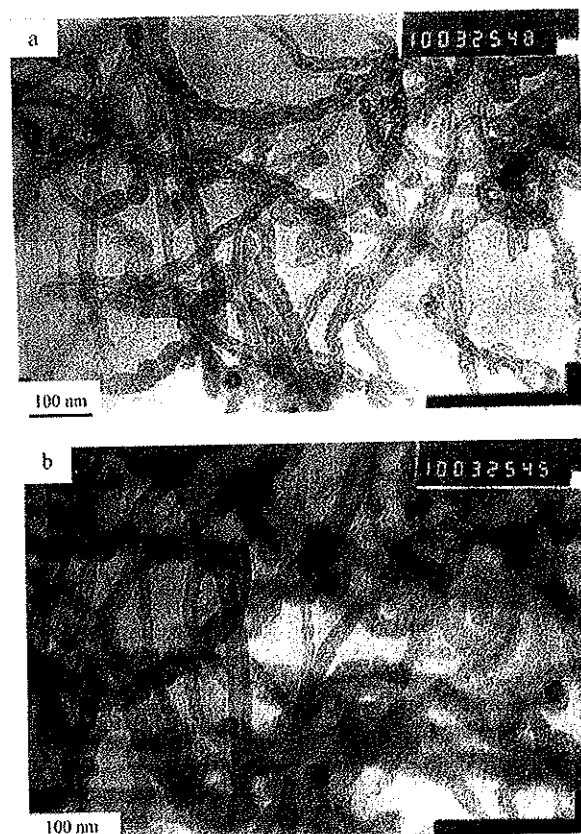


**Figure 4.** TEM photographs of (a) raw MWCNTs and (b) PBA-encapsulated MWCNTs after Soxhlet extraction for 72 h with acetone.

**Table 1. Polymer Content in Polymer-Encapsulated MWCNTs Calculated by TGA Method**

	polymer content
PBA-encapsulated MWCNTs before Soxhlet extraction	11.5%
PBA-encapsulated MWCNTs after Soxhlet extraction	7.6%
PMMA-encapsulated MWCNTs before Soxhlet extraction	2.3%
PMMA-encapsulated MWCNTs after Soxhlet extraction	1.4%

noted that after 72-h Soxhlet extraction with acetone, ~3.9 wt % unencapsulated poly(*n*-butyl acrylate) and ~1.9 wt % unencapsulated poly(methyl methacrylate) can be removed respectively from the original PBA/MWCNTs composite and PMMA/MWCNTs composite. Also, it can be found that for PBA system there is a ~7.6 wt % of encapsulation rate, which is much higher than that for the PMMA system (only ~1.4 wt %). This result can be attributed to the low conversion of MMA monomer and relatively low hydrophobic properties of MMA compared to BA monomer.

FTIR spectra of raw MWCNTs, PBA-encapsulated MWCNTs, and PMMA-encapsulated MWCNTs are shown in Figure 6. It can be noted that even after 72 h of Soxhlet extraction with boiling acetone, the characteristic peaks of PBA or PMMA can be found in the spectra of polymer/carbon nanotubes composite. The characteristic peak of C=O in carbonyl groups of PBA and PMMA at ~1733 cm<sup>-1</sup> is clear in the PBA/

(18) Xia, H. S.; Wang, Q.; Liao, Y.Q.; Xu, X.; et al. *Ultrason. Sonochem.* 2002, 9, 151.

(19) Liao, Y. Q.; Wang, Q.; Xia, H.S.; Xu, X.; et al. *J. Polym. Sci. Part A: Polym. Chem.* 2001, 39, 3356.

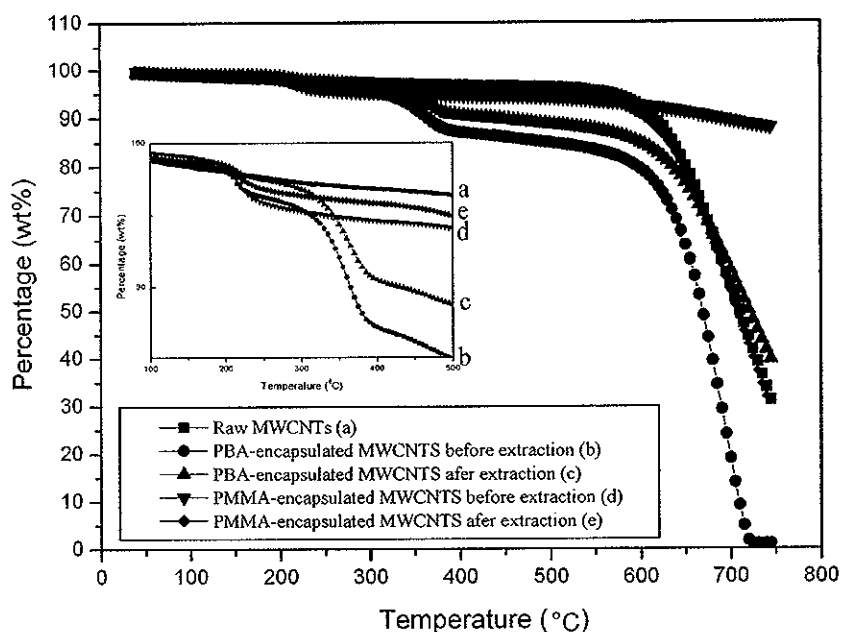


**Figure 5.** TGA curves of (a) raw MWCNTs, (b) PBA-encapsulated MWCNTs before soxhlet extraction, (c) PBA-encapsulated MWCNTs after Soxhlet extraction, (d) PMMA-encapsulated MWCNTs before soxhlet extraction, and (e) PMMA-encapsulated MWCNTs after Soxhlet extraction.

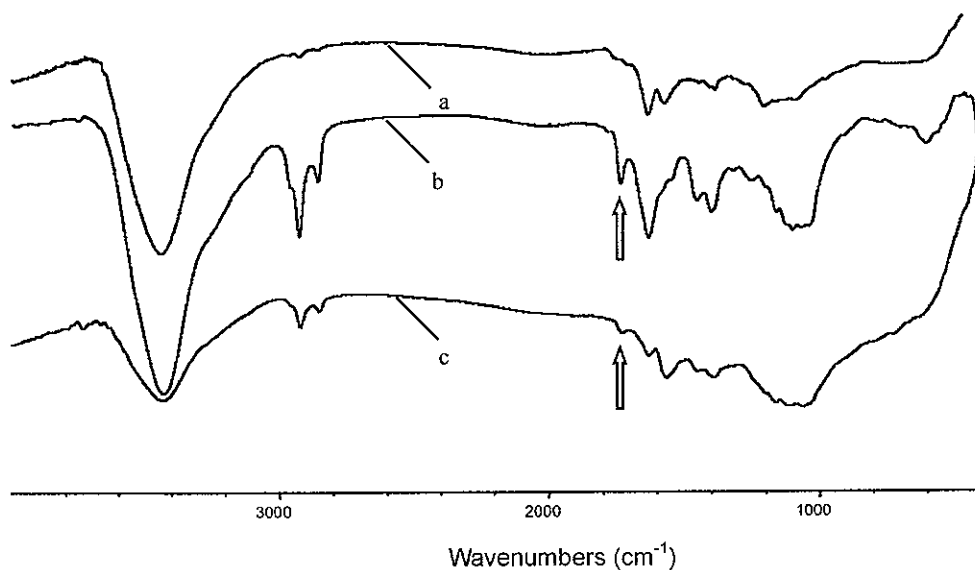


**Figure 6.** FTIR spectra of (a) raw MWCNTs, (b) PBA-encapsulated MWCNTs, and (c) PMMA-encapsulated MWCNTs after 72 h-Soxhlet extraction with acetone.

MWCNTs and PMMA/MWCNTs composites. The two peaks at  $\sim 2923\text{ cm}^{-1}$  and  $\sim 2854\text{ cm}^{-1}$  corresponding to the stretch mode of C–H bond vibration are strengthened for extracted PBA-encapsulated MWCNTs and PMMA-encapsulated MWCNTs. The peaks at  $\sim 1454\text{ cm}^{-1}$  and  $\sim 1390\text{ cm}^{-1}$  in curves b and c were attributed to the bend vibration of  $-\text{CH}_2$  or  $-\text{CH}_3$  group of polymer. The peaks at  $1000\text{--}1200\text{ cm}^{-1}$  were attributed to the stretching vibration of the C–O group of the polymer. The results suggest that the composites are not the simple mixtures of polymer and carbon nanotubes. There should be strong interaction between them. In contrast to PMMA-encapsulated MWCNTs, PBA-encapsulated MWCNTs have stronger peaks at  $\sim 1733\text{ cm}^{-1}$ ,  $\sim 2923\text{ cm}^{-1}$ , and  $\sim 2854\text{ cm}^{-1}$ , which suggests that

the interaction between PBA and carbon nanotubes is stronger.

XPS was used to investigate the surface chemical state of the obtained polymer-encapsulated MWCNTs and determine the evidence of surface encapsulation by ultrasonically initiated in-situ emulsion polymerization. Survey X-ray photoelectron spectra of the raw MWCNTs, PBA-encapsulated MWCNTs, and PMMA-encapsulated MWCNTs are shown in Figure 7. The narrow scan spectra of the C region are shown in Figure 8 and the narrow scan spectra of the  $\text{O}_{1s}$  region are shown in Figure 9. Table 2 summarizes the binding energy and the composition of every element in the surface. The ratios of the atom number of O and C (O/C) on the surface of polymer/MWCNTs composites are determined

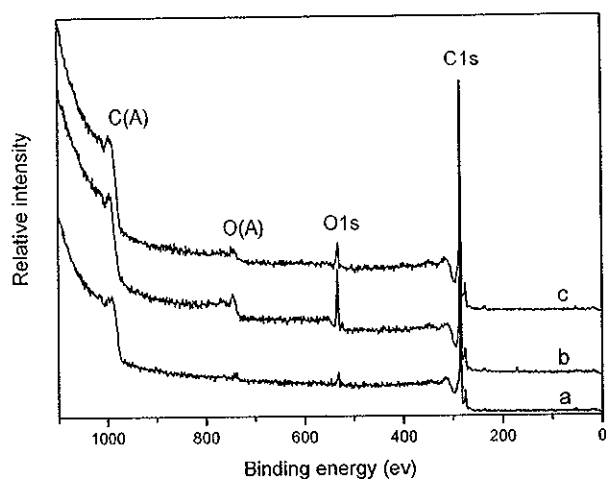


**Figure 7.** Survey X-ray photoelectron spectra of (a) raw MWCNTs, (b) PBA-encapsulated MWCNTs, and (c) PMMA-encapsulated MWCNTs after 72-h Soxhlet extraction with acetone.

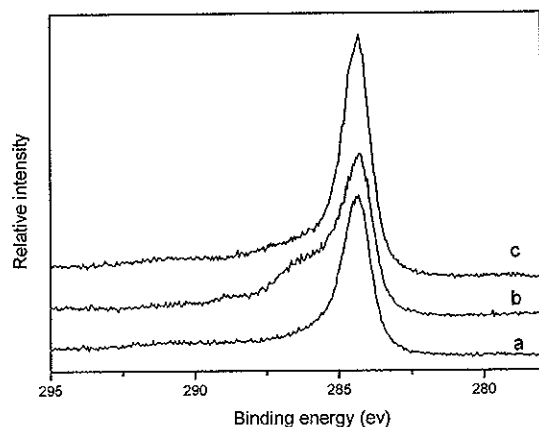


**Figure 8.**  $C_{1s}$  narrow-scan X-ray photoelectron spectra of (a) raw MWCNTs, (b) PBA-encapsulated MWCNTs, and (c) PMMA-encapsulated MWCNTs after 72-h Soxhlet extraction with acetone.

from the O/C ratios of peak areas corrected with the empirical sensitivity factors. The O/C ratios for raw MWCNTs, extracted PBA-encapsulated MWCNTs, and extracted PMMA-encapsulated MWCNTs are 0.0288, 0.1186, and 0.0493, respectively. Compared to raw MWCNTs, the enhanced oxygen signals for the extracted PBA-encapsulated MWCNTs and PMMA-encapsulated MWCNTs confirm the presence of polymer. The O/C ratios in the surface of extracted PBA-encapsulated MWCNTs and PMMA-encapsulated MWCNTs are much higher than that in the surface of the simple mixture PBA/MWCNTs with a corresponding composition of 7.6% PBA and 92.4% MWCNTs ( $O/C \approx 0.0146$ ) and the simple mixture PMMA/MWCNTs with a corresponding composition of 1.4 wt % PMMA and 98.6% MWCNTs ( $O/C \approx 0.00364$ ), respectively. The results confirm that they are not simple mixtures of polymer and MWCNTs but polymer-encapsulated MWCNTs. The O/C ratios in the surface of extracted PBA-encapsulated MWCNTs and PMMA-encapsulated MWCNTs were lower than that in the PBA ( $O/C \sim 0.286$ ) and PMMA ( $O/C \sim 0.4$ ), which suggests that some parts of the encapsulating polymer layers are thinner than the

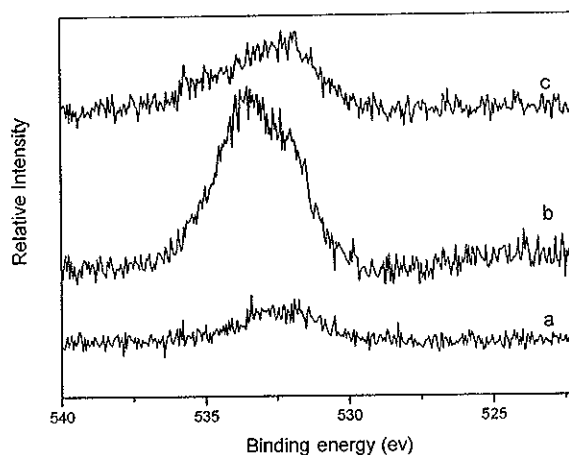


**Figure 9.**  $O_{1s}$  narrow-scan X-ray photoelectron spectra of (a) raw MWCNTs, (b) PBA-encapsulated MWCNTs, and (c) PMMA-encapsulated MWCNTs after 72-h Soxhlet extraction with acetone.

**Table 2. Binding Energy and the Composition of Every Element in the Surface of Raw MWCNTs, PBA-Encapsulated MWCNTs, and PMMA-Encapsulated MWCNTs**

element	MWCNTs		PBA-encapsulated MWCNTs		PMMA-encapsulated MWCNTs	
	BE	At%	BE	At%	BE	At%
$C_{1s}$	284.3	97.2	284.3	89.4	284.3	95.3
$O_{1s}$	532.3	2.8	533.5	10.6	532.3	4.7

interpenetrating depth of XPS ( $\sim 10$  nm) or the encapsulation is not complete; this is in agreement with the TEM results. A lower O/C ratio was found in the PMMA-encapsulated MWCNTs compared to the PBA-encapsulated MWCNTs, this should be attributed to low conversion and low encapsulation rate, which is consistent with the TGA and FTIR results.

So, by taking advantage of the multiple effects of ultrasound, i.e., dispersion, pulverizing, activation, and initiation, the aggregation and entanglement of carbon nanotubes in aqueous solution could be broken down, while in situ polymerization of monomer on the surface of MWCNTs proceeds without any added chemical initiator; consequently, the MWCNTs are coated by the formed polymer. The formation mechanism of polymer-encapsulated carbon nanotubes was proposed as illustrated in Figure 10. The process can be considered to occur in five steps. Step one is the dispersion of carbon nanotubes in aqueous solution under ultrasonic irradiation. Initially the carbon nanotubes should be well dispersed in the aqueous phase, and coagulation of CNTs during the emulsion polymerization must be avoided, because this leads to irreversible fixation of the coagulates. This is a key step for successful encapsulation. Step two is the formation of admicelle by the adsorption of surfactant layers onto the surface of the carbon nanotubes. The admicelle was defined as adsorbed micelle.<sup>20,21</sup> Because of the hydrophobic feature of carbon nanotubes, the hydrophobic chain of surfac-

(20) O'Haver, J. H.; Jeffrey, H. H.; Evans, L. R.; Waddell, W. H. *J. Appl. Polym. Sci.* 1996, 59, 1427.

(21) Aertds, A. M.; van Herk, A. M.; Klumperman, B.; Kurja J.; German, A. L. Emulsion Polymerization. In *Synthesis of Polymers*; Schlüter, A. D., Ed.; Wiley VCH: Verlag GmbH, D-69469 Weinheim, Germany, 1999; Chapter 9, p 298.

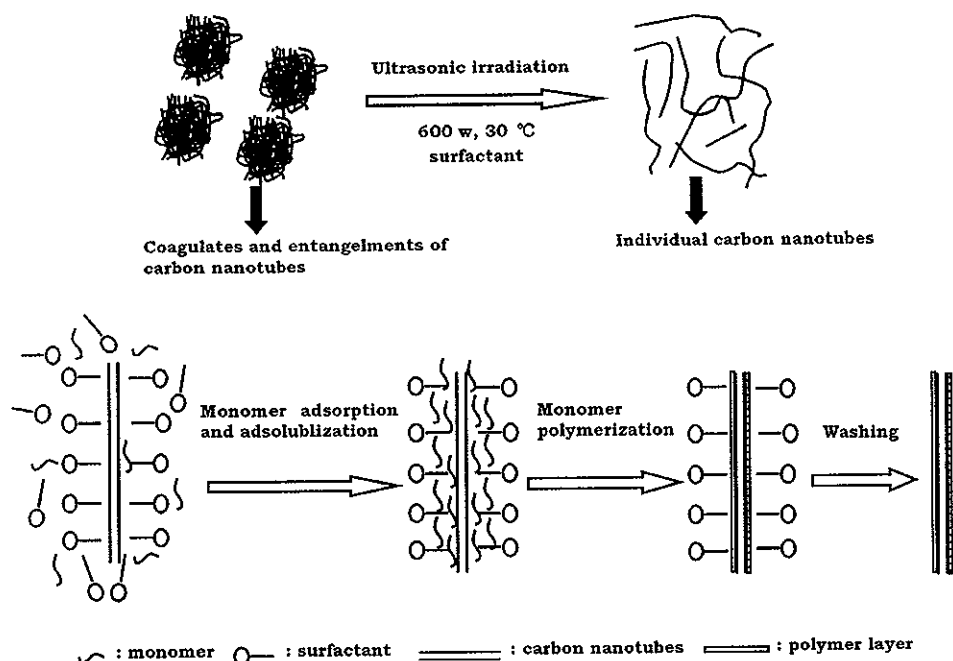


**Figure 10.** Proposed formation mechanism of polymer-encapsulated carbon nanotubes through ultrasonically initiated in-situ emulsion polymerization.

tant will anchor on the surface of carbon nanotubes. Step three is adsorption and adsolubilization of monomer. When organic monomers are introduced into the system, they preferentially partition into the interior of the admicelle. In this study, compared to MMA monomer, the relatively hydrophobic monomer BA will more easily enter into the admicelle. This is one reason for the high encapsulation rate and strong interaction for BA monomer. Step four is the in-situ polymerization of monomer. The radicals are generated by decomposition of solvent, monomer, or surfactant, or rupture of polymer chains under ultrasonic cavitation and are diffused into the admicelle to initiate the polymerization of monomer. Step five is washing of the treated powder to remove the excess surfactant with plenty of hot water to get solid polymer-encapsulated carbon nanotubes powder. To improve the encapsulation efficiency, polymerization occurs in the micelles formed by self-aggregation of surfactant molecular should be avoided to a maximum extent; this can be attained through decreasing the concentration of surfactant.

**Nylon 6/Carbon Nanotubes Composites.** Polymer-encapsulated carbon nanotubes can find many applications in many fields.<sup>9</sup> In this case we examined the reinforcing effect of MWCNTs in Nylon 6 (PA6) matrix. Nylon 6/carbon nanotubes composite is a promising engineering material that can be used in automobile parts. We employed the prepared polymer-encapsulated carbon nanotubes to prepare PA6/carbon nanotubes composites. The purpose was to improve the dispersion of carbon nanotubes in PA6 and interfacial adhesion between PA6 and carbon nanotubes. SEM photographs of the cryogenically fractured surface in liquid nitrogen of PA6/1% raw carbon nanotubes and PA6/PBA-encapsulated carbon nanotubes are shown in Figure 11. The white dots represent the ends of the carbon nanotubes in the fractured surface. Clearly, compared to PA6/1% raw carbon nanotubes (Figure 11 a), distribution of

**Table 3. Mechanical Properties of PA6/Carbon Nanotubes Composites**

	yield strength (MPa)	Young's modulus (MPa)	elongation at break (%)	tensile strength (MPa)	notched Izod impact strength (kJ/m <sup>2</sup> )
PA6	45	1336	235	62	6.1
PA6/1% raw CNTs	50	1510	188	50	4.6
PA6/1% PBA-encapsulated CNTs	59	1797	133	59	4.1

carbon nanotubes in PA6/PBA-encapsulated carbon nanotubes (Figure 11 b and c) is more uniform, and the size of carbon nanotubes in PA6/PBA-encapsulated carbon nanotubes is larger. The fact that the dispersion of PBA-encapsulated carbon nanotubes in PA 6 matrix can be improved should be attributed to two points: (i) the polymer layer introduces a steric repulsive force between the carbon nanotubes, which overcomes the van der Waals attractive force between the carbon nanotubes. (ii) The introduction of a polyacrylate layer raises the surface energy of MWCNTs and improves the compatibility between MWCNTs and Nylon 6. The mechanical properties of PA6, PA6/1% raw carbon nanotubes, and PA6/PBA-encapsulated carbon nanotubes were determined, and the results are summarized in Table 3. It can be noted that at only 1 wt % charged content of polymer-encapsulated carbon nanotubes the yield strength is improved ~31% from 45 to 59 MPa and the Young's modulus is improved ~35% from 1336 to 1797 MPa; this is attributed to good dispersion and the improved interfacial adhesion, as well as the good mechanical properties of CNTs. Also, it can be noted that with the addition of carbon nanotubes, the elongation at break and toughness of PA6/carbon nanotubes composites both decreased. The encapsulation treatment of carbon nanotubes improves the Young's modulus and

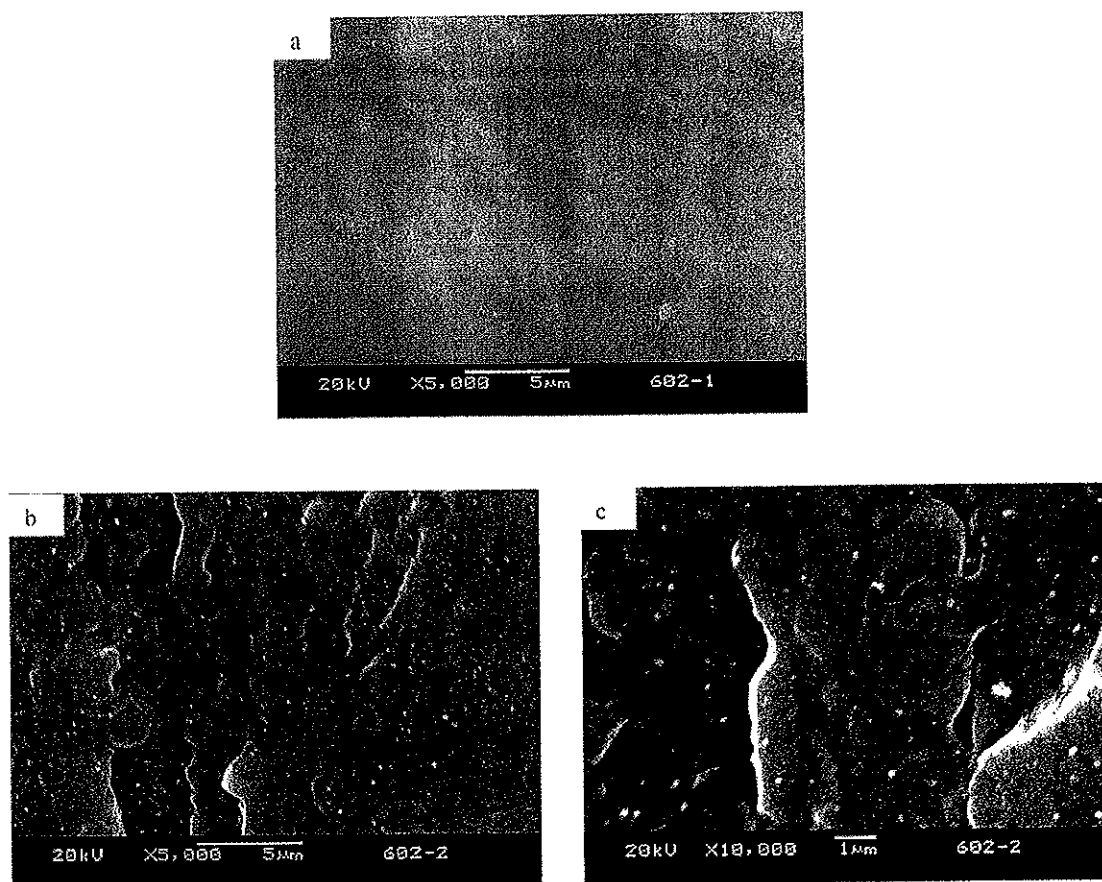


**Figure 11.** SEM photographs of cryogenically fractured surface in liquid nitrogen for (a) PA6/1% raw MWCNTs; (b) and (c) PA6/1% PBA-encapsulated MWCNTs.

the yield strength, but does not enhance the elongation and toughness of the materials. Because of their one-dimensional structure with a length of several micrometers, carbon nanotubes with good dispersion can act as bridges between the macromolecules and form weak physical cross-linking networks if there is no further treatment of orientation, thus increasing the modulus and yield strength. However, the weak physical cross-linking effect can make materials more brittle and decrease the toughness and elongation of the composite. The reasons are under further investigation.

### Conclusions

Ultrasonic irradiation has an excellent dispersion effect on carbon nanotubes in aqueous solution, and under ultrasonic cavitation radicals can be generated to initiate the polymerization without any added initiator. By employing dispersion, pulverizing, activation, and initiation functions resulted from ultrasound cavitation, the aggregation and entanglement of carbon nanotubes can be broken down. The in-situ emulsion polymerization of monomer BA or MMA proceeds while

carbon nanotubes are redispersed by ultrasound; consequently, the carbon nanotubes are coated by the synthesized polymer. Ultrasonically initiated in-situ emulsion polymerization provides a novel surface modification method for carbon nanotubes with high surface energy and much entanglement. This approach can be extended to other monomer/carbon nanotubes systems. The polymer-encapsulated carbon nanotubes can find many applications in many fields. In this case the polymer-encapsulated carbon nanotubes can be well dispersed in Nylon 6 matrix. The interface adhesion between polymer-encapsulated carbon nanotubes and Nylon 6 is improved. At only 1% charged content of polymer-encapsulated carbon nanotubes, the yield strength is improved ~31% and the Young's modulus is improved ~35% for Nylon 6/MWCNTs composites.

**Acknowledgment.** This work was supported by the National Natural Science Foundation of China (29974020, 200340061) and Ministry of Education of China.

CM0341890